

# Analysis of spider silk in native and supercontracted states using Raman spectroscopy

Z. Shao<sup>a</sup>, F. Vollrath<sup>a,\*</sup>, J. Sirichaisit<sup>b</sup>, R.J. Young<sup>b</sup>

<sup>a</sup>Department of Zoology, Aarhus University, Universitetsparken B135, DK 8000 Aarhus C, Denmark

<sup>b</sup>Materials Science Center, UMIST/University of Manchester, Grosvenor Street, Manchester M1 7HS, UK

Received 17 March 1998; revised 28 May 1998; accepted 10 June 1998

## Abstract

Well-defined, fluorescence-free Raman spectra were obtained from native as well as treated (supercontracted) major ampullate dragline silks reeled from four very different spiders: *Araneus diadematus*, *Nephila edulis*, *Latrodectus mactans* and *Euprosthenoops* sp. Conformational sensitive regions were assigned in the spectra. Compared to the silk of the silkworm *Bombyx mori*, all spider silks showed less  $\beta$ -sheet and more random coil and/or  $\alpha$ -helix material. Polarized spectra suggested that the molecular chains of the spider silk were aligned parallel to the axis of the fibre. The differences in the mechanical properties between the native and supercontracted silks were attributed to variations in  $\beta$ -sheet content. The mechanism of contraction of spider silks in solvents was correlated to conformational changes in the supermolecular structure. © 1999 Elsevier Science Ltd. All rights reserved.

**Keywords:** Fibres; Conformations; Biomechanics

## 1. Introduction

Our understanding of the microstructure of spider silk, especially the dragline of the golden silk spider *Nephila* is progressing rapidly [1–14]. For a full picture we need to use many different techniques such as n.m.r. [2–4], X-ray diffraction and scattering [5–9], TEM [9–12], LM [13], SEM [13] and AFM [14]. Important additional data come from the mechanical behaviour of silks under specific environmental conditions such as stretching [15,16] or supercontraction in water [17,18] and other solvents [13,19].

Raman spectroscopy is particularly useful for studying the conformation of proteins [20] both in the opaque solid state and in solutions. It allows us to follow conformational changes, which occur in the transition from one state to another, such as denaturation, chemical modification and crystallization. Several lepidopteran silks and their constituent polypeptides were studied using Raman spectroscopy. Visible light excitation Raman spectra of *Bombyx mori* silk were compared to the spectra of two  $\beta$ -sheet polypeptides: poly(Ala-Gly) and poly(Ser-Gly). This has established these polypeptides as model compounds for the amide I, amide III and skeletal vibrations of silk fibroin [21]. Further, the mechanical denaturation process of *Bombyx* silk fibroin

while under tensile stress was studied using Raman spectroscopy [22,23]. In addition, Fourier transform Raman spectra of several insect silk samples were published and compared with each other including the cocoons of cultivated *Bombyx*, silk from the wild Tussah moth as well as raw silk and processed silk cloth [24]. Stress-induced Raman band shifts in *Bombyx* silk have recently been obtained by R. Young (unpublished results). The only publication [25] so far on the Raman spectra of a spider silk (i.e. *Nephila clavipes* dragline silk) presents data about the structure of this silk which is rather surprising in the light of the present state of knowledge about *Bombyx* silk. In particular, the data suggests that the proportions of secondary structure in the two types of fibres are very similar [25]. However, it is not inconceivable that the methods used affected the data, i.e. both silks had been treated in 0.1% NaOH solution and/or the accuracy of spectral measurements might have been affected by silk luminescence.

In this paper, we present and discuss Raman spectra of the major ampullate silks of four rather different spiders: *Araneus diadematus*, *Nephila edulis*, *Latrodectus mactans* and *Euprosthenoops* sp. As well as comparing the spectra of the four silks to each other, as control we also compared them to our spectrum of *Bombyx mori* silk. We further obtained Raman spectra of these four spider silks contracted in a range of solvents and inferred the conformational changes

\* Corresponding author.

caused by these treatments. The results, we trust, will help our understanding of the relationships between the structure and properties of spider silks generally because: (i) the silks studied come from very different spider taxa; and (ii) these same silks were studied before [20] for their biomechanical properties under environmental conditions which included submersion in the solvents used in the present study.

## 2. Materials and methods

We used five different types of silk: four dragline silks from web spiders and one cocoon silk from a lepidopteran insect.

The spider silks were reeled from *Araneus diadematus* (Araneidae), *Nephila edulis* (Tetragnathidae), *Latrodectus mactans* (Theridiidae) and *Euprosthrops* sp. (Pisauridae). These spiders belong to different families and are genetically separated by many million years. They all build webs: *Araneus*, a garden cross spider from Europe and *Nephila*, a subtropical and moist-tropical golden silk spider from Australia are orb web-weavers, *Latrodectus*, a subtropical black widow from North America builds a tangle web and *Euprosthrops*, a dry-tropical nursery spider from Africa builds a sheet web. All spiders were raised in the laboratory and fed on house flies. Major ampullate dragline (MA) silks of the four spiders *Araneus*, *Nephila*, *Latrodectus*, and *Euprosthrops*, were reeled directly from restrained but fully-awake spiders at  $2 \text{ cm s}^{-1}$  drawing speed and under room conditions (about  $25^\circ\text{C}$  and 50% RH) [17]. The silks were collected and restrained on small plastic frames ( $10 \times 10 \text{ cm}$ ) and studied within a week of collection.

Using hard nail varnish (Elisabeth Arden, USA) sections of the collected silks were transferred (using a micro-manipulator) either to dividers, Raman frames or to SEM stubs. The spider silks had diameters of about  $2\text{--}3 \mu\text{m}$ , measured in a JEOL 840 SEM at magnification around  $3000\times$  [19]. Silk on the dividers (with an extension/relaxation screw) were submerged either into: (i) distilled water; (ii) methanol (AR); or (iii) 8M aqueous urea solution. Some of these silks were further allowed to contract to different degrees while kept under slight tension. The shrinkage of a fibre in a solvent was defined as the difference between the initial length of the fibre and its final length divided by its initial length. After contraction, the diameter of all silks increased. It should be noted that after contraction in 8M urea solution, silks were very soft, and easily broken by surface tension of the solution when taken out of the bath. To remove residual urea these silks were washed thoroughly with distilled water. The insect silk (from the silkworm *Bombyx mori* provided by the Department of Macromolecular Science, Fudan University, China) was degummed by removing the sericin on the surface of the cocoon silk using Yamaura's method [26].

For the Raman measurements single filaments, about  $10 \mu\text{m}$  thick, were glued on to the viewing frame. Spectra

of individual fibres were obtained using a Renishaw 1000 Raman microscope. The  $632.8 \text{ nm}$  red line of a He–Ne laser was focused to give  $1 \text{ mW}$  of energy on a  $2 \mu\text{m}$  spot at the surface of the fibre. Spectral data was accumulated for a  $100 \text{ s}$  period at a fixed grating position and collected using a Peltier-cooled CCD camera. This gave a Raman spectrum over an approximately  $1000 \text{ cm}^{-1}$  window for each exposure. The Raman spectra were recorded as a series of data points in the form of intensity as a function of a Raman wavenumber. Each spectrum takes the form of a background and a series of peaks. Repeat Raman measurements for the specimens demonstrated that there were no signs of structural deterioration during the measurement period; thus, exposure of the silk fibres to the laser beam did not appear to damage the fibres under the conditions employed.

## 3. Results and discussion

### 3.1. Background

Spider and insect silk are poly(amino acid)s of high molecular weight ( $M_n = 3 - 7 \times 10^5 \text{ gmol}^{-1}$ ) [27,28]. Since it does not have bioactivity, silk is not the typical active protein but rather a biosynthetic polypeptide. Consequently, it should be possible to apply our knowledge and understanding of synthetic polypeptide secondary structure to the analysis of silk structure.

Raman spectra obtained from a range of homo-poly (amino acid)s show characteristic conformational bands assigned the same vibrational mode, at slightly different positions depending on the variety of the amino acids [29]. It is not surprising that in some cases silk which contains a range of amino acids as a co-poly(amino acid) shows overlapping conformational bands in its Raman spectrum. Thus, a qualitative analysis of Raman spectra can help in the understanding of the secondary structure of silk and enable us to follow conformational changes in silk induced by different treatments. Quantitative analysis routines are available for protein secondary structure such as the widely-used Williams method which is advantageous for the study of small polypeptides [30,31]. However, this method is at present not suitable for silk fibres because all of the 15 basis set proteins used by Williams [30] were globular proteins, with the exception of poly-L-lysine, whereas the silk investigated in this present study is a fibrous protein.

The major limitation of the Raman technique for the study of proteins and some synthetic polymers, is the problem of fluorescence leading to strong backgrounds and consequently poor spectral quality. In our study the use of a red He–Ne laser produced well defined, fluorescence-free spectra. Thus, the position of the bands and their arbitrary intensities are well defined. For each of the Raman spectra obtained, the band at about  $1450 \text{ cm}^{-1}$  associated with the  $\text{CH}_2$  bending modes was used as an intensity standard, since it is insensitive to the conformation of the protein [32,33].

Nevertheless, it is meaningless to use the intensity of bands for quantitative comparison of the conformations of silks of different species, since: (i) the absolute intensity of the  $1450\text{ cm}^{-1}$  band is expected to be proportional to the number of  $\text{CH}_2$  groups; and (ii) the amino acid composition has not been determined for some of the silks studied here. Thus, for meaningful conformational comparisons between different silk fibres, we compared the ratios of relative peak height intensities of two bands (e.g.  $1652\text{ cm}^{-1}$  and  $1669\text{ cm}^{-1}$ ) in the same spectrum.

### 3.2. Comparison between bombyx and spider silks

Fig. 1 compares the Raman spectra of two benchmark silks: the MA silk of the spider *Nephila* and the cocoon silk of the moth *Bombyx*. For all our measurements we kept the direction of polarization of the laser radiation either fully parallel or fully perpendicular to the long axes of the silk fibres. Several important conclusions can be drawn from the spectra obtained. A previous study [24] noted significant differences between the Raman spectrum of a single silkworm fibre and that of the bulk material (e.g. a silkworm cocoon or processed silk cloth). In contrast, our observations on single *Bombyx* fibres showed identity between the spectrum of single fibre (Fig. 1b) and fibre bundles reported previously [22–24], suggesting mainly  $\beta$ -sheet structure for degummed silkworm silk.

The spectra of typical spider silk (Fig. 1a) and degummed silkworm silk (Fig. 1b) differed considerably. We note that the spectra of parallel and perpendicular orientation of spider silk show at least two distinct  $n(\text{CO})$  amide I bands. The peak in  $1669\text{ cm}^{-1}$  is characteristic of  $\beta$ -sheet/ $\beta$ -turn

configuration for the polypeptide backbone [29] and agrees very well with assignments made for some other proteins containing a high proportion of these configurations [34]. The lower wavenumber peak around  $1652\text{ cm}^{-1}$  (missing in silkworm silk) might indicate the existence of an  $\alpha$ -helical configuration [35,36] and/or random coil [37]. The spider silk spectra further showed either a distinct band or a shoulder peak centered near  $1683\text{ cm}^{-1}$  (see also Fig. 2), which suggests that a monohydrogen-bonded or disordered helix [30] might be present also in spider silks.

The intermediate region from  $1450\text{ cm}^{-1}$  to  $1200\text{ cm}^{-1}$  was similar in all the samples studied, except for two small differences: (i) the spectral band at  $1450\text{ cm}^{-1}$  in *Bombyx* silk was shifted to a higher wavenumber in *Nephila* silk; and (ii) in the perpendicular spectrum of the spider silk, the amide III band appeared at  $1247\text{ cm}^{-1}$  instead of at  $1230\text{ cm}^{-1}$  as found in the parallel spectrum. The band at  $1247\text{ cm}^{-1}$  in *Bombyx* silk is thought to arise from random coils [23,24,38] and other polypeptides [39], while the band at  $1230\text{ cm}^{-1}$  was found to be associated with either a disordered configuration in *Bombyx* [24] or a  $\beta$ -conformation in synthetic polypeptides [29,40].

Below  $1200\text{ cm}^{-1}$ , we note additional differences between spider and insect silks: spider silk had a  $1095\text{ cm}^{-1}$  band whereas in silkworm silk the band appeared at  $1085\text{ cm}^{-1}$ ; spider silk had an additional peak at  $907\text{ cm}^{-1}$ . The  $1095\text{ cm}^{-1}$  band might be regarded as the compromise of all conformations in spider silk, because the  $1085\text{ cm}^{-1}$  band was assigned as a disordered configuration of the  $n(\text{CC})$  skeletal band of polypeptide chain [24]. If the polypeptide chains were in the form of  $\alpha$ -helices [21,41,42] or  $\beta$ -sheets [33] this band would appear at  $1108\text{ cm}^{-1}$  or

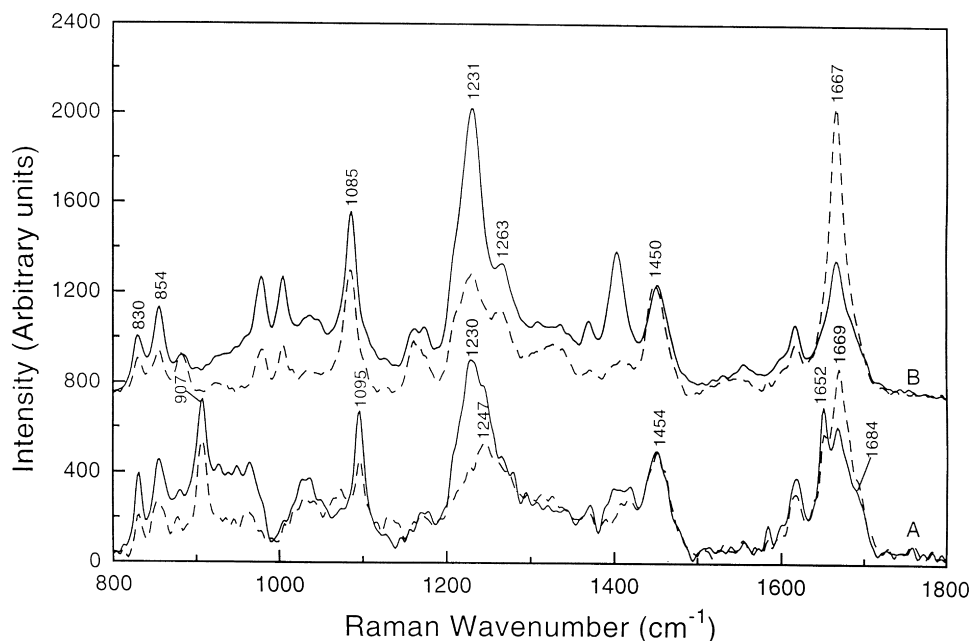


Fig. 1. Raman spectra of: (A) major ampullate silk of *Nephila edulis*; and (B) degummed silk of *Bombyx mori*. A single fibre was aligned either parallel (solid line) or perpendicular (dashed line) to the direction of polarization of the laser beam. The wavenumbers and vibrational assignments of Fig. 1b can be found in [24].

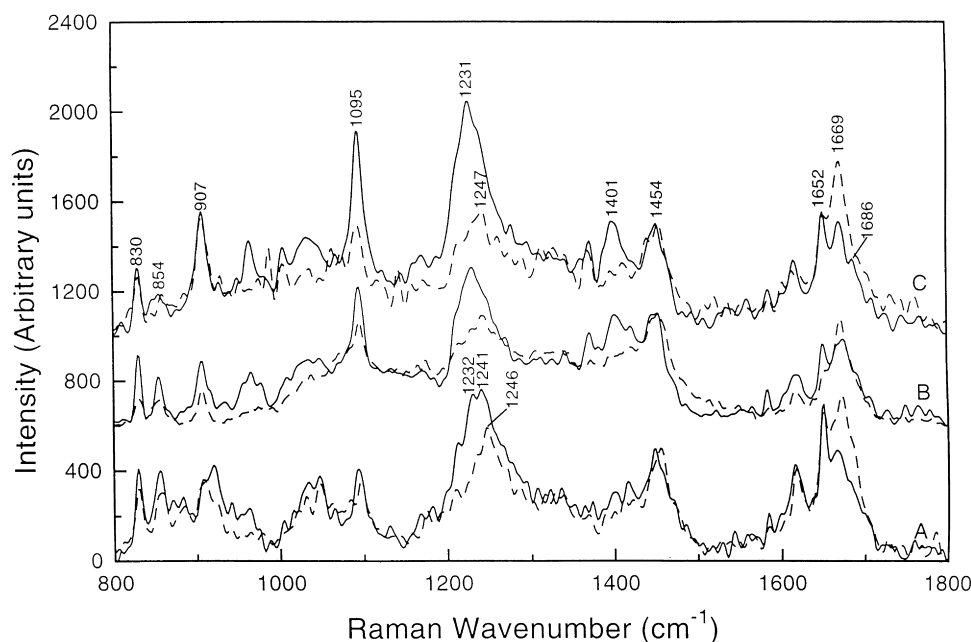


Fig. 2. Raman spectra of major ampullate silks of: (A) *Araneus diadematus*; (B) *Euprosthonops* sp.; and (C) *Latrodectus mactans* in their natural states. The fibres aligned as for [1].

1078  $\text{cm}^{-1}$ , respectively. We were surprised to find a band at 907  $\text{cm}^{-1}$  in spider silk not present in the silkworm silk. Still, although the ratios of amino acids (especially for proline) are quite different between spider and silkworm silk, both have similar amino acid presence [43]. The 907  $\text{cm}^{-1}$  band, which may be assigned to the  $\text{C}'\text{-CH}_3$  stretching mode, also appears in the spectrum of poly(L-Alanine) [39] but not in spectra of poly(Ala-Gly) and poly(Gly-Ser) [21]. Thus, this particular peak suggests and possibly confirms that spider dragline silks have a motif of  $(\text{Ala})_n$  ( $n = 4\text{--}7$ ) [44,45], rather than the Ala-Gly-Ala-Gly-Ser-Gly repeat found in *Bombyx* silk.

Fig. 2 shows the Raman spectra of major ampullate silks of *Araneus* (a), *Latrodectus* (b) and *Euprosthonops* (c); the spectrum of *Nephila* silk was shown in Fig. 1. We note that

there were no significant differences in Raman spectra between the four spider silks, other than the intensity ratio of 1652  $\text{cm}^{-1}$  to 1669  $\text{cm}^{-1}$  bands (Table 1) and the amide III band of *Araneus* silk splitting into a double peak at 1230  $\text{cm}^{-1}$  and 1242  $\text{cm}^{-1}$  in the parallel spectrum. This suggests that the spider silks studied by us had similar amino acid compositions and concentrations and, hence, similar secondary structures. However, on a higher level of order, the relative intensities of the 1652  $\text{cm}^{-1}$  and 1669  $\text{cm}^{-1}$  bands for the different silks seemed to suggest that *Euprosthonops* silk had the highest level of  $\beta$ -sheet conformation and *Araneus* silk had the least, while the level was nearly the same for the *Nephila* and *Latrodectus* silks. This might indicate that *Araneus* silk contains a higher level of random coil conformation than the other spider silks.

Table 1

Relative intensity ratios of the Raman bands 850 to 830  $\text{cm}^{-1}$  and 1669 to 1652  $\text{cm}^{-1}$  for the silks studied. (Tyr = Tyrosine content with<sup>a</sup> notes, references; State = condition: native or superconducted, s. % = superconducted in %)

Silk	Treatment	I(850)/I(830) parallel	I(850)/I(830) perpendicular	I(1669)/I(1652) parallel	I(1669)/I(1652) perpendicular	Tyr
<i>Bombyx</i>	control	1.50	1.23			5.2[46]
<i>Araneus</i>	control	0.98	0.90	0.71	1.10	1.0[47]
	s.15% in H <sub>2</sub> O	0.79	0.86	0.54	0.92	
	s.35% in H <sub>2</sub> O	0.68	0.77	0.49	0.72	
<i>Nephila</i>	control	1.35	1.29	0.88	1.40	2.9[48]
	s.14% in CH <sub>3</sub> OH	1.26	1.23	0.85	1.09	
	s.28% in H <sub>2</sub> O	1.24	0.93	0.59	0.80	
	control urea	1.45	1.06			
	s.40% in urea	1.96	2.52			
	s.60% in urea	2.08	1.85			
<i>Latrodectus</i>	control	0.62	0.71	0.92	1.45	
<i>Euprosthonops</i>	control	0.69	0.86	1.06	1.92	

<sup>a</sup>Expressed as residues per 100 total residue.

We further note that some of the spectral bands (Fig. 1 and Fig. 2) were highly polarized. The band at  $1230\text{ cm}^{-1}$  shifted to  $1247\text{ cm}^{-1}$  and the relative intensities of some bands (e.g. at  $1667\text{ cm}^{-1}$ ,  $1404\text{ cm}^{-1}$ ,  $1230\text{ cm}^{-1}$ ,  $1250\text{ cm}^{-1}$  and  $1095\text{ cm}^{-1}$ ) in the parallel spectra differed from those of the perpendicular spectra. Specifically, for each spider silk the intensity ratio of  $1669\text{ cm}^{-1}$  to  $1652\text{ cm}^{-1}$  was much greater in spectra perpendicular rather than parallel to the fibre axis (see Table 1). Considering the vibrational assignments of silk [24], the spectra confirm that the  $\beta$ -sheets and partially ordered regions in all the silk fibres are highly oriented along the fibre axis. Furthermore, the band at  $1230\text{ cm}^{-1}$  is more likely to be attributable to a  $\beta$ -sheet structure and/or other oriented backbone chains such as a  $3_1$ -helix rather than a random coil. Otherwise, because of the high symmetry of the disordered polypeptide chains, there should be no difference between the Raman spectra obtained with different polarizations of the laser beam.

### 3.3. Conformational changes of spider silk after contraction in solvents

Spider silks were shown to shrink in water [17,18], and in a range of polar solvents such as methanol, ethanol and urea solutions [19]. We now discuss the conformational changes occurring in spider silks during such solvent induced contractions.

#### 3.3.1. Contraction in water and methanol

The Raman spectra of *Araneus* silk unshrunk (A-control) and shrunk by 15% (B); and 35% (C) in water are shown in Fig. 3 for the fibre both in parallel and perpendicular

orientation to the polarization of the laser beam. Both the relative intensities and peak positions of the Raman bands changed with increasing contraction of the silk. The ratio of the intensity of the  $1669\text{ cm}^{-1}$  to  $1652\text{ cm}^{-1}$  bands was reduced in the amide I region (Table 1). This suggests that the proportion of the  $\beta$ -conformation decreased significantly with silk contraction. In the amide III region, the  $1230\text{ cm}^{-1}$  band ( $\beta$ -sheet) shifted to a higher wavenumber on contraction and a peak appeared at  $1272\text{ cm}^{-1}$  (probably associated with the  $\alpha$ -helix [23] and/or random coil [37]). There was a general tendency for the parallel and perpendicular spectra to be very similar although there were a few differences. They all show that, after contraction, the amount of  $\beta$ -conformation material appeared to decrease and random coil and/or helix structure increased, the molecular chains remaining parallel to the fibre axis.

The Raman spectra of *Nephila* silk contracted in both methanol and water show a similar trait (Fig. 4). The 14% and 28% shrinkage values represent the limitation of *Nephila* silk shrinkage in methanol and water, respectively [19]. The changes in spectra seem to follow the same behaviour compared with *Araneus* silk contracted in water. We note that, rather than shifting during contraction, the  $1230\text{ cm}^{-1}$  band splits into a double peak at  $1229\text{ cm}^{-1}$  and  $1243\text{ cm}^{-1}$  and decreases in intensity. This might indicate that a reasonable amount of  $\beta$ -conformation remains while, at the same time, some molecules are transformed into random coils and  $\alpha$ -helices. Moreover, the spectra were almost identical for *Nephila* silk contracted in methanol and *Araneus* silk in the native (i.e. untreated) state (cf. Fig. 3a and Fig. 4b). The different mechanical properties, particularly the elongation at failure (about 25% for *Araneus* silk and more than 50% for contracted *Nephila* silk in our

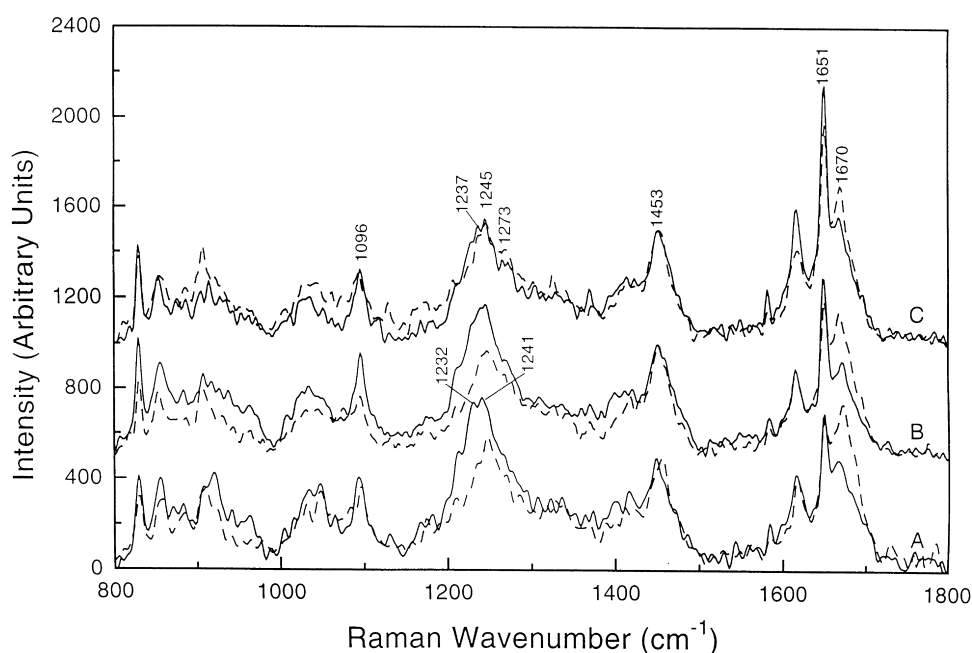


Fig. 3. Raman spectra of *Araneus diadematus* silk: (A) control; (B) contracted 15% in water; and (C) contracted 35% in water. The fibres aligned as for [1].

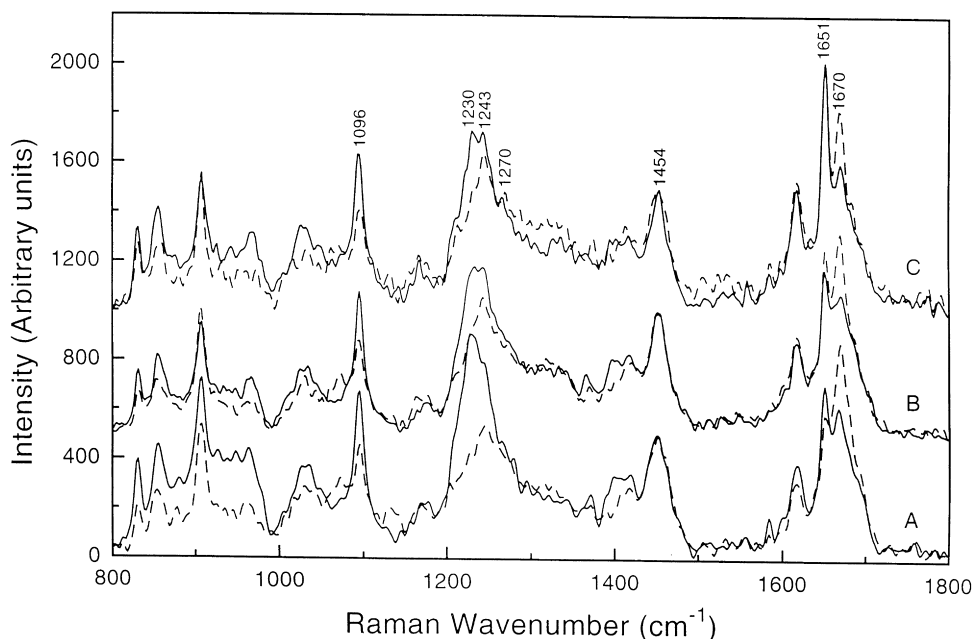


Fig. 4. Raman spectra of *Nephila edulis* silk: (A) control; (B) shrunk 12% in methanol; and (C) shrunk 28% in water. The fibres aligned as for [1].

measurements) suggest strongly that to understand the mechanical properties of spider silks fully, it is necessary to know not only the diversity of secondary structures but also a number of other variables, such as the dimensions of these structures and the orientations of the molecular chains.

Proteins containing tyrosyl residues are known to give Raman spectra with a doublet at 850 and 830  $\text{cm}^{-1}$  [42,49,50]. It was demonstrated [42] that the intensity ratio of these two peaks is sensitive to the nature of the hydrogen bonding of the phenyl hydroxyl group or its ionization, and much less to the environment of the phenyl ring, as earlier assumed [51]. The ratio  $I(850)/I(830)$  is reduced going from moderately to strongly hydrogen-bonded tyrosines [37]. Table 1 shows that for both *Araneus* and *Nephila* silk, the decreasing value of the ratio of these two peaks correlates with the contraction of the silk, both in water or methanol. This implies that the tyrosyl residues in these silks are more strongly hydrogen-bonded after contraction. This could be explained by the fact that contraction in the solvent may induce the molecular chains in the silk to change from the well-ordered  $\beta$ -conformation to less-organized random coil and/or helix structures.

### 3.3.2. Contraction in urea

In 8M urea the silks of *Euprosthenoops*, *Latrodectus* and *Nephila* underwent contraction by about 20%, 25% and more than 60%, respectively, while still retaining some structural integrity [13,19]. *Araneus* silk, on the other hand, supercontracted by more than 50% but at the same time disintegrated (unpublished observations). We suggest that all four silks were attacked by the urea and partially dissolved because the silk surfaces developed bubble-like protuberances after submersion in 8M urea solution (unpublished observations by S. Z. and F.V. on *Nephila* silk using

AFM). Fig. 5 shows the Raman spectra of restrained *Nephila* silk immersed in 8M urea solution and allowed to shorten between 40%–60% of its initial length. In this silk, when compared to the native *Nephila* silk (Fig. 1), some of the bands changed considerably with contraction (Fig. 5). For example, the Amide I band shifted to lower wavenumbers and it was difficult to distinguish the doublet after contraction. Also, the Amide III band moved from 1230  $\text{cm}^{-1}$  and split into two bands at  $\sim 1245 \text{ cm}^{-1}$  and  $\sim 1265 \text{ cm}^{-1}$ , in both the parallel and perpendicular spectra. This suggests that many new random coils were formed during the process of contraction and disintegration. The band in 1095  $\text{cm}^{-1}$  shifted to 1102  $\text{cm}^{-1}$  for 40% shrinkage and to 1105  $\text{cm}^{-1}$  for 60% shrinkage. This strongly suggests that the contraction led also to an increase in  $\alpha$ -helix conformations. Additional evidence for the existence of  $\alpha$ -helix conformation in contracted spider silk comes from a new broad peak that appeared in the spectra at around 1336  $\text{cm}^{-1}$ . This could be a sensitive method of characterizing synthetic polypeptides in the  $\alpha$ -helix form [52,53]. However, the ratio of  $I(850)/I(830)$  in the spectra from urea-contracted silk (Table 1) increased with increasing contraction whereas in water or methanol the ratio decreased with increasing contraction. It is hard to explain this behaviour solely in terms of conformational changes of the silk molecular chains. It might be that the highly-concentrated urea solution disintegrates part of the silk, as mentioned earlier. Thus, the constitution of contracted silk would be different from the original material, causing an unexpected change of the ratio of  $I(850)/I(830)$  (i.e. the environment of the tyrosyl residues).

## 4. Conclusions

This study has shown that Raman spectroscopy provides

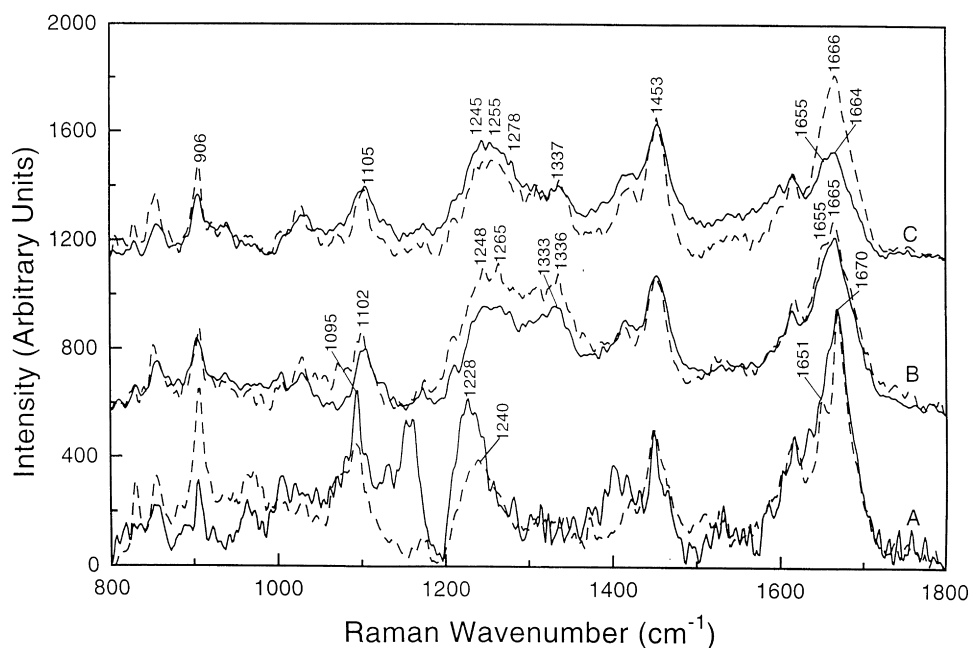


Fig. 5. Raman spectra of *Nephila edulis* silk submerged in 8M urea solution: (A) control, submerged but not shrunk because restrained at both ends [19]; (B) shrunk 40%; and (C) shrunk 60%. The fibres aligned as for [1].

a valuable tool for investigating the molecular nature of spider silks as well as insect silks, especially when well-defined, fluorescence-free Raman spectra can be obtained. We conclude from our spectra that the secondary structures of spider and *Bombyx* silks are very different. This contradicts conclusions from earlier Raman spectroscopy studies [25]. Our results indicate that: (i) the  $\beta$ -conformation is less prevalent in spider MA silk than in silkworm silk; and (ii) native MA spider silk has low levels of random coil and/or  $\alpha$ -helix conformations comparing the contracted silk (note that we could not distinguish between random coil or  $\alpha$ -helix and  $3_1$ -helix formations [3] in the Raman spectra). It is not surprising that spider silks with more random coil and/or  $\alpha$ -helix conformations are generally much tougher than the silkworm silk with a structure dominated by  $\beta$ -sheets [19]. Indeed, the differences in secondary structure can be used in the interpretation of biomechanical data even between different spider silks from data [19] showing that the dragline silk of *Araneus* is relatively weak while the silk of *Euprostheno*s is significantly stiffer. This is consistent with the Raman results suggesting that *Araneus* silk has a lower level of  $\beta$ -conformations than *Euprostheno*s silk.

It is only logical to assume that the contraction of dragline silk in solvents is accompanied by conformational changes in the molecular chains. This assumption would support the hypothesis that supercontraction of spider silks is the result of the rupture of hydrogen bonds and changes in the orientation and coiling of molecular chains [9]. Obviously, the longitudinal contraction and lateral swelling of a silk fibre in a given solvent is likely to depend on the degree of crystallinity of the bulk material (i.e. the proportion of  $\beta$ -sheet stacking) and on the ability of solvent to interact with the

proteins. A reduction in the strength of hydrogen bonds in polar solvents may allow the protein to take up a less extended conformation [19].

### Acknowledgements

ZS thanks the Carlsberg Foundation for a generous Post-doctorate fellowship. FV and ZS thank the Danish Research Foundation (SNF) for support. JS thanks the Government of Thailand for financial support. The work in Manchester is part of a large program of research upon fibres and composites supported by the British Engineering and Physical Sciences Research Council. The authors thank Dr. David Knight for editorial comments on the manuscript.

### References

- [1] Kaplan DL, Adams WW, Farmer B, Viney C. Silk polymers—materials science and biotechnology, ACS Symposium Series 544. Washington, DC: ACS, 1994.
- [2] Simmons AH, Ray E, Jelinski LW. *Macromolecules* 1994;27:5235.
- [3] Kümmerlen J, Beek JD, Vollrath F, Meier BH. *Macromolecules* 1996;29:2920.
- [4] Simmons AH, Michal CA, Jelinski LW. *Science* 1996;271:84.
- [5] Grubb DT, Jelinski LW. *Macromolecules* 1997;30:2860.
- [6] Parkhe AD, Seeley SK, Gardner K, Thompson L, Lewis RV. *J Mol Recognition* 1997;10:1.
- [7] Bram A, Branden CC, Snigireva I, Riekel C. *J Appl Cryst* 1997;30:390.
- [8] Yang Z, Grubb DT, Jelinski LW. *Macromolecules* 1997;30:8254.
- [9] Thiel BL, Kunkel DD, Viney C. *Biopolymers* 1994;34:1085.
- [10] Thiel BL, Viney C. *MRS Bull* 1995;20:52–56.

- [11] Thiel BL, Viney C. *J Microscopy* 1997;185:179–187.
- [12] Frische S, Maunsbach AB, Vollrath F. *J Microscopy* 1998;189:64.
- [13] Vollrath F, Holtet T, Thogersen HC, Frische S. *Proc R Soc Lond* 1996;B263:147.
- [14] Li SFY, McGhie AJ, Tang SL. *Biophys J* 1994;66:1209.
- [15] Termonia Y. *Macromolecules* 1994;27:7378.
- [16] Kitagawa M, Kitayama T. *J Mater Sci* 1997;32:2005.
- [17] Work RW, Emerson PD. *J Arachnol* 1982;10:1.
- [18] Work RW. *J Exp Biol* 1985;118:379.
- [19] Shao Z, Vollrath F. *Polymer*, in press.
- [20] Tu AT. *Raman spectroscopy in biology: principles and applications*. New York: Wiley, 1982.
- [21] Frushour BG, Koenig JL. *Biopolymers* 1975;14:2115.
- [22] Magoshi J, Magoshi Y, Nakamura S. *Polym Commun* 1985;26:309.
- [23] Zheng S, Li G, Yao W, Yu T. *Appl Spectrosc* 1989;43:1269.
- [24] Edwards HGM, Farwell DW. *J Raman Spectrosc* 1995;26:901.
- [25] Gillespie DB, Viney C, Yager P. *Silk polymers — materials science and biotechnology*, ACS Symposium Series 544. Washington, DC: ACS, 1994:155.
- [26] Yamaura K, Okumura Y, Matsuzawa S. *J Macromol Sci Phys* 1982;B21:49.
- [27] Shimura K, Akai H, Iizuka E, Garel J-P, Ikekawa N. *Experientia* 1983;39:441.
- [28] Jackson C, O'Brien JP. *Macromolecules* 1995;28:5975.
- [29] Xue G. *Prog Polym Sci* 1994;19:317.
- [30] Williams RW. *J Mol Biol* 1983;166:581.
- [31] Williams RW. *Meth Enzym* 1986;130:311.
- [32] Frushour BG, Koenig JL. *Biopolymers* 1974;13:1809.
- [33] Yu T-J, Lippert JL, Peticolas WL. *Biopolymers* 1973;12:2161.
- [34] Williams AC, Barry BW, Edwards HGM. *Analyst* 1994;119:563.
- [35] Barry BW, Williams AC, Edwards HGM. *Spectrochim Acta* 1993;A49:801.
- [36] Williams AC, Edwards HGM, Barry BW. *J Raman Spectrosc* 1994;25:95.
- [37] Monti P, Freddi G, Bertoluzza A, Kasai N, Tsukada M. *J Raman Spectrosc* 1998;29:297.
- [38] Ito K, Magoshi J, Magoshi Y, Nakamura S. In: *Proceedings of Sixth International Conference on Raman Spectroscopy*, Vol. 2, 1978:290.
- [39] Fanconi B, Small EW, Peticolas WL. *Biopolymers* 1971;10:1277.
- [40] Lord CR, Yu NT. *J Mol Biol* 1970;50:509.
- [41] Itoh K, Oya M. *Polymer J* 1986;18:837.
- [42] Siamwiza MTM, Lord RC, Chen MC, Takamatsu T, Harada I, Matsuura H, Shimanouchi T. *Biochemistry* 1975;22:2474.
- [43] Wainwright SA, Biggs WD, Currey JD, Gosline JM. *Mechanical design in organisms*. Princeton, NJ: Princeton University Press, 1982.
- [44] Lewis RV. *Acc Chem Res* 1992;25:392.
- [45] Guerette PA, Ginzinger DG, Weber BHF, Gosline JM. *Science* 1996;272:112.
- [46] Lucas F, Rudall KM. Extracellular fibrous proteins: the silks. In Florin M, Stotz EH, editors. *Comparative biochemistry*, vol. 26B. Amsterdam: Elsevier, 1968:475.
- [47] Peakall DB. *J Expl Zoology* 1964;154:345.
- [48] Lombardi SJ, Kaplan DL. *J Arachnol* 1990;18:297.
- [49] Chen MC, Lord RC. *Biochemistry* 1899;1976:15.
- [50] Pezolet M, Pigeon-Gosselin M, Coulombe L. *Biochimica Biophys Acta* 1976;453:502.
- [51] Yu N-T, Jo BH, O'Shea DC. *Arch Biochem Biophys* 1973;156:71–76.
- [52] Koenig JL, Sutton P. *Biopolymers* 1970;9:1229.
- [53] Koenig JL, Sutton P. *Biopolymers* 1971;10:89.